

## III.4

# A CASE OF COMPLEX MATTER: COEXISTENCE OF MULTIPLE PHASE SEPARATIONS IN CUPRATES

G. Campi and A. Bianconi

*Department of Physics, University of Rome “La Sapienza”, P.le Aldo Moro 2, 00185 Rome, Italy*

**Abstract:** A modified Van der Waals scheme for cuprates to give the co-existence of multiple phase separations in cuprates is presented. The model includes the tendency of charge carriers to form anisotropic directional bonds at preferential volumes for the formation of different “liquid phases”. We obtain the variation of the pseudogap temperature  $T^*(\delta)$  (for phase separation between pseudogap matter and normal matter) with hole density ( $\delta$ ) in agreement with experiments. We discuss the thermodynamic parameters that control the variation of the phase diagram of different cuprate families.

**Key words:** Multiple Phase Separation, Spinodal Lines, Cuprates

PACS numbers 64.75.+g, 81.30.Mh, 74.72.-h

## 1. INTRODUCTION

The problem of phase separation in cuprates superconductors has been longly debated [1-8]. Recently, several experiments show the formation of electronic crystals at critical densities [9, 10]. These results provide a strong experimental support for the scenario proposed some years ago (11-14) for the phase diagram of cuprate superconductors where generalized Wigner

polaron crystals are formed at critical values of the charge densities, i.e., at integer values of the filling factor.

The critical densities for the formation of the electronic polaronic crystals depend on the effective volume occupied by the doped charge carriers. The anisotropic interactions between the doped charge carriers produce the stripe or checkboard phases [15-16].

The van der Waals scheme is the simplest scheme to describe the spinodal phase separation that has been used to describe the co-existence of a polaronic gas (low density insulating phase) and a polaronic liquid (high density metallic phase) by Emin [1], or for more complex phase separation models including magnetic interactions [2-3].

In order to give account of the new emerging complex phase diagram of cuprates, where different phases coexist, we have extended the model of Poole et al. [17] for supercooled water.

## 2. THE MODEL

We use a modified Van der Waals interaction model, analogously to the one introduced for the phase diagram of supercooled water [17]. In fact, supercooled water, a prototype of complex matter, shows a phase separation driven by the tendency of water molecules to form arrays of hydrogen bonds. This tendency gives fluctuating clusters made of a low density liquid (LDL) that coexists with the high density liquid water (HDL). In order to describe this anomalous phase separation in water, the model of Poole et al. [47] implements the standard Van der Waals model by including a characteristic gain in energy “ $\gamma$ ” for the formation of clusters with directional hydrogen bonds at a particular preferential volume “ $V_\gamma$ ”. The introduction of this anisotropic interaction provides a phase diagram with the coexistence of a high density liquid (HDL) and a low density liquid (LDL) when  $\gamma$  is larger than a threshold value [47].

Here we have extended the Poole model in order to describe multiple phase separations in cuprates. The free energy of a complex system in which  $n$  phase separations are observed, is obtained by adding the term  $A_\gamma$  to the Van der Waals free energy  $A_{VDW}$  yielding a total free energy

$$A = A_{VDW} + A_\gamma \quad (1)$$

where  $A_{VDW}$  and  $A_\gamma$  are given by

$$A_{VDW} = -RT \left\{ \ln \left[ \frac{V-b}{\Lambda^3} \right] + 1 \right\} - \frac{a}{V^2} \quad (2)$$

$$A_\gamma = -RT \sum_{i=1}^{n-1} f_i \ln [\Omega_i + \exp(-\gamma_i/RT)] - \left[ 1 - RT \sum_{i=1}^{n-1} f_i \ln(\Omega_i + 1) \right] \quad (3)$$

Here  $a$  and  $b$  are the standard Van der Waals constants. The Van der Waals constant  $a$  is associated with the isotropic inter-particle attraction. Each intermediate phase,  $i$ , is characterized by the anisotropic inter-particle interaction  $\gamma_i$ . In this approach, for each phase  $i$  there are  $\Omega_i \gg 1$  configurations all having  $\gamma_i = 0$  and only a single configuration in which the formation of the anisotropic bonds with energy  $\gamma_i$  is allowed.

The anisotropic interaction, characteristic of the intermediate phase  $i$ , is most likely to occur when the bulk molar volume is consistent with a preferential volume  $V_{\gamma_i}$ . In fact, each particle has an optimal local volume for the formation of anisotropic bonds to its neighbours. Changing the particle density, when  $V \neq V_{\gamma_i}$ , the anisotropic interactions are only a fraction  $f_i$  of the total, since  $V$  is no longer consistent with the possibility that all anisotropic interactions are saturated at the optimal volume. The remaining fraction of bonds,  $1-f_i$ , occurs in an unfavourable local volume and therefore, they cannot form the anisotropic bonds of the  $i$  phase.

The term  $f_i$  is given by

$$f_i = \exp \left\{ -[(V - V_{\gamma_i})/\sigma_i]^2 \right\} \quad (4)$$

where  $\sigma_i$  characterizes the width of the region of volume around  $V_{\gamma_i}$  over which a significant fraction of anisotropic bonds can be described by Eq. (3).

To describe the phase diagram of cuprates, where we observe four phase separations, we consider a Poole model with three different anisotropic interactions  $\gamma_1$ ,  $\gamma_2$ , and  $\gamma_3$  giving rise to three different intermediate phases with preferential volume  $V_{\gamma_1}$ ,  $V_{\gamma_2}$  and  $V_{\gamma_3}$  respectively.

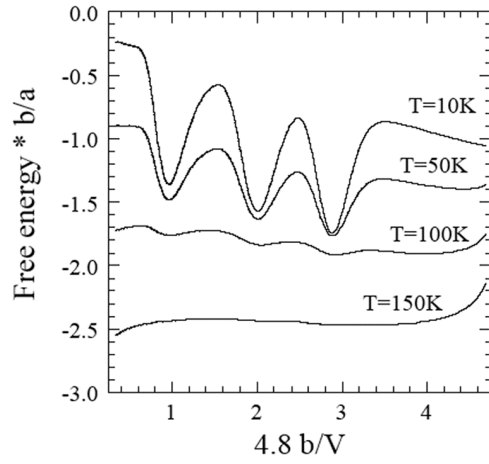


Figure III:4:1. The Helmholtz free energy as a function of reduced density at different temperatures. In this way the minima of the free energy in Fig. 1 occur at the reduced density, or filling factor 1, 2 and 3. These new minima, indicating the occurrence of three intermediate phases at different densities, become deeper when the temperature decreases, as shown in Fig. 1 for  $T=10\text{K}$ ,  $50\text{K}$ ,  $100\text{K}$  and  $150\text{K}$ . The occurrence of these new intermediate phases is also shown in Fig. 2 where we have plotted the state equation with pressure  $P$  as a function of reduced density, at the same temperatures  $T = 10\text{K}$ ,  $50\text{K}$ ,  $100\text{K}$  and  $150\text{K}$ .

The values of the parameters  $a, \sigma_v, \gamma_i, \Omega_i$  are fixed to get a qualitative agreement with experimental data. For the standard Van der Waals model we have chosen  $a=1.2 \text{ Pa m}^6/\text{mol}^2$ , with  $\gamma_0=a/b=6 \text{ KJ/mol}=62 \text{ meV}$  and  $b=2.00 \cdot 10^{-4} \text{ m}^3/\text{mol}$ . We have selected  $b$  in such a way that the particle effective volume is a sphere with radius  $r=4.3 \text{ \AA}$ . For the first intermediate phase we use  $|\gamma_1|=6.75 \text{ KJ/mol}=70 \text{ meV}$ ,  $V_{\gamma 1}=9.35 \cdot 10^{-4} \text{ m}^3/\text{mol}$  and  $\sigma_1=V_{\gamma 1}/4$ . For the second intermediate phase we use  $|\gamma_2|=6.75 \text{ KJ/mol}=70 \text{ meV}$ ,  $V_{\gamma 2}=4.81 \cdot 10^{-4} \text{ m}^3/\text{mol}$  and  $\sigma_2=V_{\gamma 2}/7$ , while for the third intermediate phase we impose  $|\gamma_3|=6.75 \text{ KJ/mol}=70 \text{ meV}$ ,  $V_{\gamma 3}=3.34 \cdot 10^{-4} \text{ m}^3/\text{mol}$  and  $\sigma_3=V_{\gamma 3}/11$ . In all intermediate phases we have chosen  $\Omega_1 = \Omega_2 = \Omega_3 = \exp(-S_{\gamma}/R)$  where  $S_{\gamma} = -70.25 \text{ J/(K mol)}$  is the entropy of formation of a mole of anisotropic bonds and  $R$  is the universal gas constant.

The inclusion in the model of three optimum volumes  $V_{\gamma_1}$ ,  $V_{\gamma_2}$  and  $V_{\gamma_3}$  for three different anisotropic bonds  $\gamma_1$ ,  $\gamma_2$  and  $\gamma_3$ , introduces three new minima in the free energy when  $V$  approaches  $V_{\gamma_1}$ ,  $V_{\gamma_2}$  and  $V_{\gamma_3}$ . In Fig. 1 we have plotted the free energy as a function of the reduced density in units of  $1/4.8b$ .

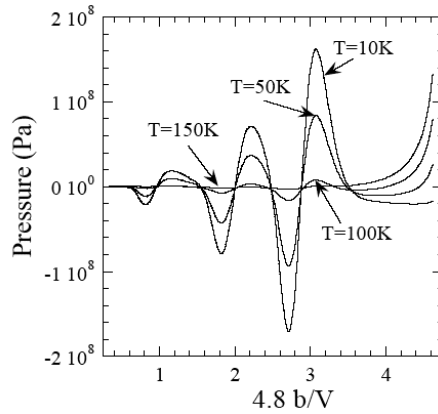


Figure III:4:2. The pressure as a function of the reduced density at different temperatures. The phase diagrams, obtained by calculating the spinodal line from Eq. 1, depend on the thermodynamic parameters described above. In Fig. 3 we report some representative phase diagrams with different anisotropic interactions.

In panel a), we have used the values above  $\gamma_0=a/b=62$  meV,  $|\gamma_1|=|\gamma_2|=|\gamma_3|=70$  meV. We observe that the effect of the  $A_\gamma$  term in Eq. 1, related to the strength of the anisotropic interactions, is to “split” the normal Van der Waals spinodal curve by imposing thermodynamic stability in the region of states centered at the reduced density 1, 2 and 3 where the three different intermediate phases are stable. As a result, four spinodal lines occur, each terminating at a critical point producing four phase separation regions. As the directional bond energies  $|\gamma_i|$  ( $i>1$ ) decrease respect with the Van der Waals interaction  $|\gamma_0|$ , the phase separations generated by the strength of the directional bonds decrease and the stabilizing effect of  $A_\gamma$  set in only at lower temperature and the critical points  $C_n$  merge with the high density spinodal of the main Van der Waals spinodal line that is formed when all  $|\gamma_i|$  go to zero (panel f).

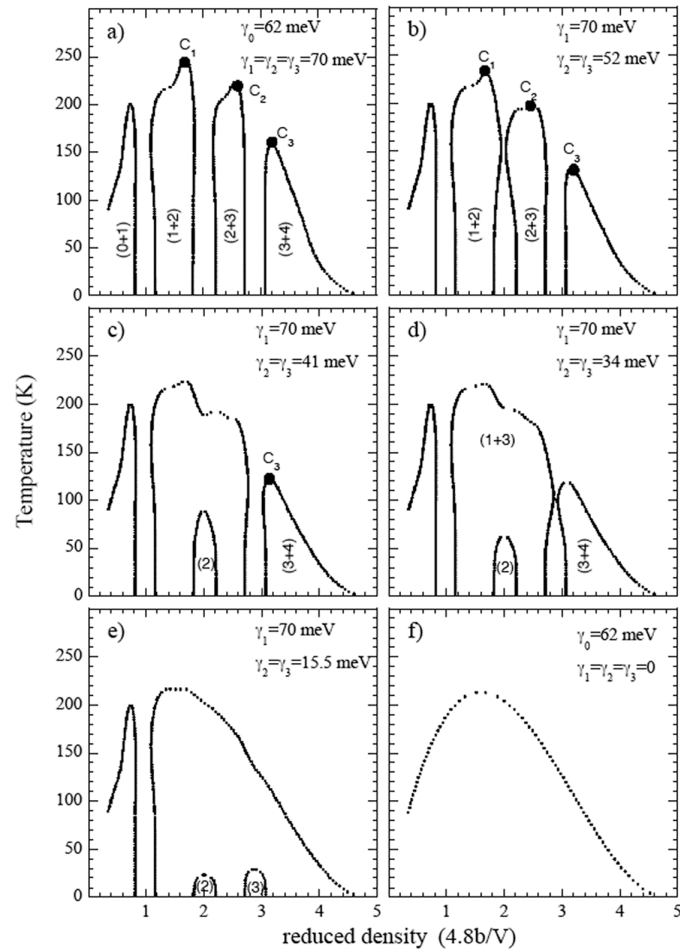


Figure III:4.3. The phase diagrams obtained by computing the spinodal lines from Eq. 1. We can observe the occurrence of four phase separations indicated by the four spinodal lines in panel a). In the panel b), c), d), e) and f) we show the effect of the strength of the directional bonds (see text)

In the following phase diagrams of panel b), c), d), e) we keep the  $\gamma_1$  value fixed ( $\gamma_1=70$  meV), while we change the  $\gamma_2$  and  $\gamma_3$  values in order to show the effects of the strength of the anisotropic interactions on the thermodynamic behaviour of the system.

In panel b) we observe that the two spinodal lines, (1+2) and (2+3), are going to overlap decreasing  $\gamma_2$  and  $\gamma_3$  ( $\gamma_2 = \gamma_3 = 52$  meV) so that the phase separation due to the thermodynamic stability centred at reduced density 2 is going to disappear below a critical value of the interaction  $|\gamma_2| = |\gamma_3| \sim 50$  meV. The disappearance of this phase separation is clearly shown in panel c) where decreasing the  $\gamma_2$  and  $\gamma_3$  interactions ( $\gamma_2 = \gamma_3 = 41$  meV) the intermediate low density phase centred at reduced density  $\rho=2$ , becomes completely enclosed within a spinodal line in which the states would otherwise be unstable. On the other hand the third intermediate phase, centred at reduced density  $\rho=3$  is stable and the phase separation (3+4) at high density is still present. If we continue to decrease the  $\gamma_2$  and  $\gamma_3$  interactions we reach the critical threshold  $\gamma_2 = \gamma_3 = 34$  meV, where also the third phase separation (3+4) merges with the one at lower density as shown in the panel d). When  $\gamma_3$  becomes less than 34 meV the third intermediate low density phase centred at reduced density  $r=3$  becomes an isolated pocket of stability completely enclosed within a spinodal line as shown in panel e), where we have used  $\gamma_2 = \gamma_3 = 15.5$  meV. In this case the action due to the central and symmetric interaction  $a$  is prevalent since  $|\gamma|$  is lower than a characteristic value, and the phase separations between the separate spinodal curves becomes two isolate “pockets” of stability at the reduced density 2 and 3 below the low temperatures 22K and 29K respectively. Finally, when the anisotropic interactions  $\gamma_1$ ,  $\gamma_2$  and  $\gamma_3$ , go to zero we reach a quantum critical point where we obtain the standard Van der Waals phase diagram shown in panel f).

### 3. THERMODYNAMIC BEHAVIOUR OF COMPLEX OXIDES

Now we apply this model to the  $\text{La}_{2-x}\text{Sr}_x\text{CuO}_4$  (LSCO) and  $\text{Bi}_2\text{Sr}_2\text{CaCu}_2\text{O}_{8+\delta}$  (Bi2212) compounds.

We report in Fig.4 the pseudo-gap temperatures  $T^*$  measured by Singer et al. [18] with the pseudo-gap temperature  $T^*$  in EXAFS experiments [19].

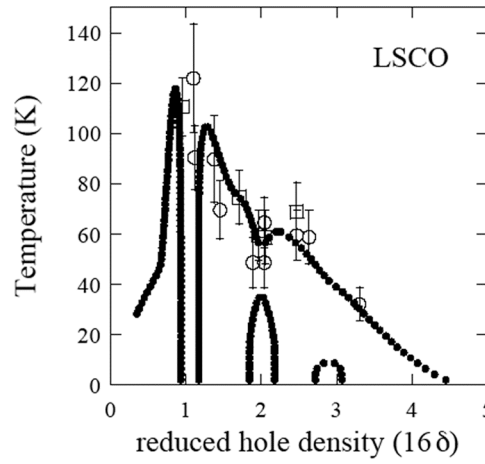


Figure III:4:4. The phase diagram for the LSCO: the open circles correspond to the  $T^*$  temperatures obtained by Singer [18]; the squares indicate the values of  $T^*$  measured by XANES spectroscopy by our group.

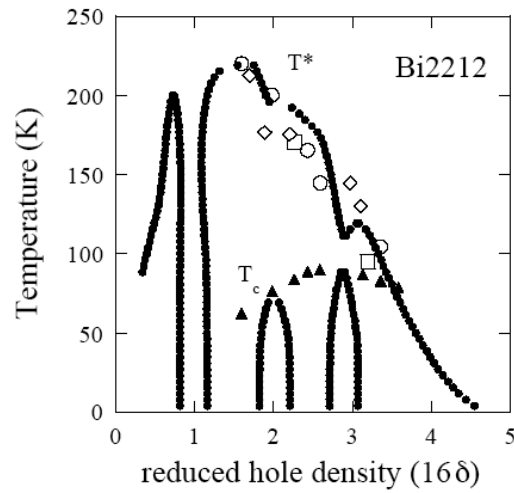


Figure III:4:5. The phase diagram for the Bi2212: the circles and the squares correspond to the  $T^*$  temperatures obtained from experiments by Oda [20] and from Arpes measurements by Ding [21] respectively; the diamonds indicate the EXAFS  $T^*$  measurements by Saini et al. [22]. The superconducting  $T_c$  are also indicated by the full triangles.



We have reproduced the experimental pseudo-gap temperature using the thermodynamic model above discussed. The phase diagram has been obtained calculating the spinodal line from Eq.1. We have imposed  $\gamma_0=a/b=19.5$  meV,  $b= 2.00 \cdot 10^{-4}$  m<sup>3</sup>/mol,  $|\gamma_1|=44$ meV,  $V_{\gamma_1}= 9.25 \cdot 10^{-4}$  m<sup>3</sup>/mol,  $\sigma_1=V_{\gamma_1}/6.25$ ,  $|\gamma_2|=14$  meV,  $V_{\gamma_2}= 4.81 \cdot 10^{-4}$  m<sup>3</sup>/mol,  $\sigma_2=V_{\gamma_2}/8.33$ ,  $|\gamma_3|=5.2$  meV,  $V_{\gamma_3}=3.34 \cdot 10^{-4}$  m<sup>3</sup>/mol,  $\sigma_3=V_{\gamma_3}/11$  and  $\Omega_1=\Omega_2=\Omega_3=\exp(-S_{\gamma}/R)$  where  $S_{\gamma}=-70.25$  J/(K mol).

In Fig. 5 we report the experimental pseudo-gap temperatures T\* for the Bi2212 system [20-21]. The calculated phase diagram has been obtained by imposing  $\gamma_0=a/b=62$  meV,  $b= 2.00 \cdot 10^{-4}$  m<sup>3</sup>/mol,  $|\gamma_1|=70$ meV,  $V_{\gamma_1}=1.00 \cdot 10^{-3}$  m<sup>3</sup>/mol,  $\sigma_1=V_{\gamma_1}/6.25$ ,  $|\gamma_2|=37$  meV,  $V_{\gamma_2}=4.81 \cdot 10^{-4}$  m<sup>3</sup>/mol,  $\sigma_2=V_{\gamma_2}/8.33$ ,  $|\gamma_3|=33$  meV,  $V_{\gamma_3}=3.34 \cdot 10^{-4}$  m<sup>3</sup>/mol,  $\sigma_3=V_{\gamma_3}/11$  and  $\Omega_1=\Omega_2=\Omega_3=\exp(-S_{\gamma}/R)$  where  $S_{\gamma}=-70.25$  J/(K mol).

In conclusion we have presented a model for an electronic complex system with coexistence of different electronic phases at critical densities and coexistence of different liquids described by the modified van der Waals model as proposed for supercooled water. We discuss the critical values of the anisotropic interactions for the spinodal lines. We find that this model is able to describe the evolution of the pseudo-gap temperature versus doping in different cuprate families.

## ACKNOWLEDGEMENTS

This work is supported by MIUR in the frame of the project Cofin 2003 "Leghe e composti intermetallici: stabilità termodinamica, proprietà fisiche e reattività" on the "synthesis and properties of new borides".

## REFERENCES

1. D. Emin, *Phys. Rev. B*, **49**, 9157 (1994); *Phys. Rev. Lett.* **72**, 1052 (1994).
2. J. C. Phillips, and J. Jung, *Phil. Mag. B* **81**, 745 (2001).
3. L.P. Gorkov in *Proc. of the Toshiba Intern. School of superconductivity* Kyoto Japan 15-20 July (1991), Springer Series in Solid State Sciences S. Maekawa, and M. Sato editors vol. 106 pag.71 Springer Verlag Berlin 1992

4. K. A. Müller, G.-M. Zhao, K. Conder and H. Keller *Journal of Physics: Condensed Matter* **10**, L291-L296 (1998); D. Mihailovic and K. A. Müller in "High- $T_C$  Superconductivity 1996: Ten Years after the Discovery", edited by E. Kaldis, E. Liarokapis and K. A. Müller (Kluwer Academic, Dordrecht 1996) NATO ASI Series vol. **343** pp. 243.
5. *Phase Separation in Cuprate Superconductors* edited by K. A. Müller and G. Benedek (World Scientific, Singapore, 1993). " (Proc. of the workshop held in Erice, Italy, 6-12 May, 1992).
6. "Phase Separation in Cuprate Superconductors" edited by E. Sigmund and A. K. Müller (Springer Verlag, Berlin-Heidelberg, 1994), (proc. of the second int. workshop on Phase Separation held in Cottbus, Germany, Sept 4-10, 1993)
7. V. Cataudella, G. De Filippis, G. Iadonisi, A. Bianconi and N. L. Saini, *Int. Jour. of Modern Physics B* **14**, 3398 (2000).
8. A. Bianconi, G. Bianconi, S. Caprara, D. Di Castro, H Oyanagi, and N. L. Saini, *J. Phys.: Condens. Matter*, **12** 10655 (2000); A. Bianconi, N. L. Saini, S. Agrestini, D. Di Castro, and G. Bianconi *Int. Jour. of Modern Physics B* **14**, 3342 (2000).
9. T. Hanaguri, C. Lupien, Y. Kohsaka, D.-H. Lee, M. Azuma, M. Takano, H. Takagi, and J. C. Davis, *Nature* **430**, 1001 (2004).
10. K.M. Shen, F. Ronning, D.H. Lu, F. Baumberger, N.J.C. Ingle, W.S. Lee, W. Meevasana, Y. Kohsaka, M. Azuma, M. Takano, H. Takagi, Z.X. Shen, *Science* **307**, 901 (2005).
11. A. Bianconi *Sol. State Commun.* **91**, 1 (1994).
12. A. Bianconi, M. Missori *Sol. State Commun.* **91**, 287 (1994).
13. A. Bianconi. *Physica C* **235-240**, 269 (1994).
14. A. Bianconi, M. Missori, H. Oyanagi, and H. Yamaguchi D. H. Ha, Y. Nishiara and S. Della Longa, *Europhysics Letters* **31**, 411 (1995).
15. F. V. Kusmartsev *Phys. Rev. Lett.* **84**, 530 (2000); *ibidem* **84**, 5026 (2000). F. V. Kusmartsev, *Europhys. Lett.* **54**, 786 (2001).
16. Anup Mishra, Michael Ma, Fu-Chun Zhang, Siegfried Guertler, Lei-Han Tang, and Shaolong Wan, *Phys. Rev. Lett.* **93**, 207201 (2004).
17. P. H. Poole, F. Sciortino, T. Grande, H. E. Stanley, and C. A. Angell, *Phys. Rev. Lett.* **73**, 1632 (1994) and references therein.
18. P. M. Singer, A. W. Hunt, A. F. Cederstro, and T. Imai, *Phys. Rev. B* **60**, 15345 (1999).
19. N. L. Saini, H. Oyanagi, Z. Wu and A. Bianconi, *Supercond. Sci. Technol.* **15**, (2002).
20. N. Momono, R. Dipasupil, G. Ishiguro, S. Saigo, T. Nakamo, M. Oda, and M. Ido, *Physica C* **317-318**, 603 (1999).
21. H. Ding, T. Yokoya, J. C. Campuzano, T. Takahashi, M. Randeria, M. R. Norman, T. Mochiku, K. Kadowaki, J. Giapintzakis, *Nature (London)* **382**, 6586 (1996).